558–565 Nucleic Acids Research, 1996, Vol. 24, No. 4

Binding to the yeast Swi4,6-dependent cell cycle box, CACGAAA, is cell cycle regulated *in vivo*

Lea A. Harrington+ and Brenda J. Andrews*

Department of Molecular and Medical Genetics, University of Toronto, Toronto, Ontario M5S 1A8, Canada

Received November 27, 1995; Accepted December 17, 1995

ABSTRACT

In *Saccharomyces cerevisiae* commitment to cell division occurs late in the G1 phase of the cell cycle at a point called Start and requires the activity of the Cdc28 protein kinase and its associated G1 cyclins. The Swi4,6-dependent cell cycle box binding factor, SBF, is important for maximal expression of the G1 cyclin and *HO* endonuclease genes at Start. The cell cycle regulation of these genes is modulated through an upstream regulatory element termed the SCB (Swi4,6-dependent cell cycle box, CACGAAA), which is dependent on both *SWI4* and *SWI6*. Although binding of Swi4 and Swi6 to SCB sequences has been well characterized *in vitro*, the binding of SBF *in vivo* has not been examined. We used *in vivo* dimethyl sulfate footprinting to examine the occupancy of SCB sequences throughout the cell cycle. We found that binding to SCB sequences occurred in the G1 phase of the cell cycle and was greatly reduced in G2. In the absence of either Swi4 or Swi6, SCB sequences were not occupied at any cell cycle stage. These results suggest that the G1-specific expression of SCB-dependent genes is regulated at the level of DNA binding *in vivo*.

INTRODUCTION

Passage through Start in *Saccharomyces cerevisiae* requires the activity of the Cdc28 kinase and the G1 cyclins, Cln1, Cln2 and Cln3 (reviewed in 1). *CLN1* and *CLN2* are periodically expressed and their protein levels also peak at Start, concurrent with maximal Cdc28 kinase activity (2,3). *CLN3*, however, is expressed at low levels throughout the cell cycle and Cln3–Cdc28 kinase activity is not significantly periodic (2). Two additional yeast G1 cyclins, *PCL1* and *PCL2* (formerly called *HCS26* and *ORFD* respectively) are also maximally expressed in G1 (2,4–6). Recent biochemical and genetic data suggest that Pcl1 and Pcl2 complex with another cyclin-dependent kinase, Pho85, to promote cell cycle progression (6,7).

Maximal expression of the G1 cyclins, *CLN1*, *CLN2*, *PCL1* and *PCL2*, at Start requires the activity of a transcription factor, SBF (SCB binding factor), which binds the repeated upstream regulatory sequence CACGAAA (SCB, Swi4,6-dependent cell cycle box) (reviewed in 8). Multiple copies of this sequence are sufficient to confer cell cycle-regulated transcription upon a reporter gene (9,10). SBF is composed of at least two proteins, Swi4 and Swi6 (4,11–13). Swi4 specifically binds the SCB sequence, whereas Swi6 binds indirectly via its interaction with the C-terminus of Swi4 (14–16). In the absence of Swi4 or Swi6 or if the SCB sequences are deleted, transcription of *HO* is abolished (11,17,18) and that of the G1 cyclins is greatly reduced (4,19–22). More recently, detailed analysis of *CLN2* transcriptional activation has suggested that other non-SCB consensus elements, which may also depend on *SWI4*, are involved in the periodic transcriptional regulation of *CLN2* (21,22).

The binding of SBF to SCB sequences has been well characterized *in vitro* (4,11,13,15). The upstream regulatory sequence, URS2, of the *HO* endonuclease gene contains 10 SCB elements (18). In gel mobility shift assays, promoter sequences from URS2 support SBF complex formation in extracts prepared from cells throughout the cell cycle (the 'L' or 'lower complex') (13; B.J.Andrews, unpublished results). In addition, a minor cell cycle-regulated complex of slightly slower mobility forms on URS2 probes and is Cdc28 dependent (the 'U' or 'upper complex') (13). Since the appearance of this upper complex occurs slightly after the transcriptional induction of *HO* and persists following *HO* repression after Start, its significance with respect to *HO* transcriptional activation is not clear (13).

A related transcription factor, the *Mlu*I cell cycle box binding factor (MBF, also called DSC1), is composed of Swi6 and the Swi4 homolog Mbp1 (20,23,24). MBF binds an upstream regulatory element (MCB, consensus ACGCGTNA) which is present in the promoters of several genes whose expression is induced at Start, including *SWI4*, the S phase cyclins *CLB5* and *CLB6* and other genes involved in DNA synthesis (23–28). The MCB element can also direct Start-specific transcription of a heterologous gene and periodic binding of MBF to MCB elements has been observed *in vitro* (25). In *Schizosaccharomyces pombe* the MBF-like complex, DSC1, also binds its target sequence in a cell cycle-regulated manner *in vitro* (29,30). So far the only *in vivo* observation to suggest that MBF and SBF DNA binding may be cell cycle-regulated is the subcellular localization of the Swi6 protein; Swi6 is nuclear throughout G1 phase and is predominantly cytoplasmic from late G1 until late M phase (13,48).

One hypothesis consistent with these data is that the SBF and MBF transcription factors modulate the cell cycle-specific

* To whom correspondence should be addressed

+Present address: Amgen Institute, 620 University Avenue, Toronto, Ontario M5G 2C1, Canada

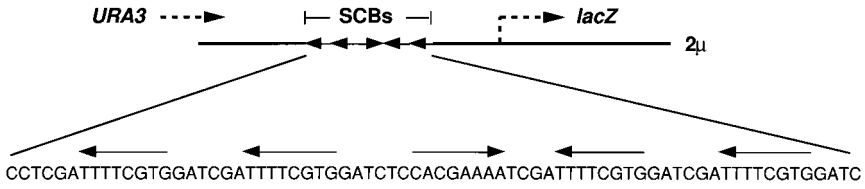

Figure 1. The promoter sequence of the SCB::*lacZ* reporter gene used in this study (11). The direction of the flanking *URA3* and *lacZ* genes are shown by a dashed arrow and the relative orientation of the SCB consensus sequences upstream of the *lacZ* gene is indicated by solid arrows. The plasmid contains a *CYC1* TATA box between the SCB elements and the *lacZ* transcription start site (41).

expression of their target genes through periodic changes in their binding activity (8,31,32). In order to examine this question directly we used *in vivo* dimethyl sulfate (DMS) footprinting to assay for SBF binding throughout the cell cycle. Our *in vivo* data support the notion that temporal regulation of SBF binding is involved in the G1-specific transcriptional induction of SCB-containing genes.

MATERIALS AND METHODS

Strains and plasmids

The following yeast strains were used for footprinting experiments: KN699 (=W303a; 2), *MAT*α *ade2-1 trp1-1 leu2-3,112 his3-11,15 ura3 can1-100* [*psi*$^+$] (Figs 2 and 6); BY105, *MAT*α *trp*Δ*63 ura3-52 lys2-801*^{a} *ade2-107*^{o} *his3*Δ*200 leu2-*Δ*1* (isogenic to JO14; 4; Fig. 3); BY210, *MAT*α *swi4*Δ*HIS3*, otherwise isogenic to BY105 (Figs 4 and 6); BY211, *MAT*α *swi6*::*HIS3*, otherwise isogenic to BY105 (Figs 5 and 6). The SCB::*lacZ* plasmid, pBA259, was constructed using synthetic SCB oligonucleotides as described (11). The plasmid carries five copies of the SCB consensus sequence upstream of a *CYC1*::*lacZ* reporter gene in vector YEp24 (Fig. 1). Yeast strains were transformed using standard techniques (33).

Cell cycle experiments

Cells were grown to a density of ~1 × 10^7 cells/ml in complete synthetic medium lacking uracil (SC-URA) (34). Except where noted, galactose was used as a carbon source and cells were grown and elutriated at room temperature. Elutriations were performed as previously described, with minor modifications (2). For loading onto the centrifugal elutriator ~2.0–4.0 × 10^{10} cells were pelleted and resuspended in ~200 ml medium (for flocculant strains, such as *swi6* deletion strains, 50 mM EDTA was included in the loading buffer). Cells were loaded at 18 ml/min into a Beckman JC-MI centrifugal elutriator (rotor type JE-5.0) at 2400 r.p.m., pre-equilibrated with the appropriate medium (for most experiments the 'conditioned' medium from the supernatant taken from the pelleted cells was used). Once cells had equilibrated within the rotor the pump speed was gradually increased by 2 ml/min every 3–5 min. The eluate was collected in 200–400 ml increments and cell size and budding were monitored microscopically and using a Coulter channelizer. Typically the first wild-type daughter cells eluted at 30–36 ml/min, whereas for the *swi4* and *swi6* deleted cells (unbudded cell size greater) the first elution peak occured at >42 ml/min. In particular, for the *swi6*Δ cells elution required both an increase in pump speed to 46 ml/min and a decrease in rotor speed to 1800 r.p.m. A maximum of 10% of the load volume could be recovered as a homogeneous population of unbudded cells. For the wild-type elutriations a total of five elutriation experiments were performed, using two different strain backgrounds (Figs 2 and 3 and data not shown); for the *swi4*Δ and *swi6*Δ strains a total of two elutriations for each strain were performed, using similar genetic backgrounds (Figs 4 and 5 and data not shown).

The synchrony in these experiments was comparable with other published reports (2), but the large sample volumes needed for DMS footprinting required pooling of G1 cuts from the elutriator. Therefore, in these experiments the percent budded indices are not an indication of the synchrony of the experiment. In addition, percent budded was measured at the time of DMS treatment and not when the sample was first removed from the elutriator. For example, the first elutriator cut from the experiment shown in Figure 2 had a modal cell volume of 17 fl; at the time the sample was DMS treated this modal cell volume had increased to 23 fl.

For each time point ~100 ml cells were used for DMS footprinting (see below), 10 ml for RNA preparation and 1 ml for FACS analysis. Total RNA was isolated, transferred to nylon membrane and probed as described (35). The probes used were: a 1.3 kbp *Xho*I–*Nco*I fragment of *CLN2* (36); a 1.0 kbp *Nde*I–*Eco*RI internal fragment of *lacZ*; a 600 bp *Eco*RI–*Hin*dIII internal fragment of *ACT1*. FACS (fluorescence-activated cell sorter) analysis was performed using software as described previously (6).

DMS footprinting

In vivo DMS footprinting was performed using a modification of published protocols (37,38). For each sample ~1 × 10^9 cells were divided in half and pelleted. Half of the sample was rinsed once in 1 M sorbitol and frozen at –20°C for subsequent DNA extraction and *in vitro* DMS modification. The remaining pellet was resuspended in 1 ml medium (SC-URA with either galactose or raffinose as appropriate). Ten microliters of DMS were added, mixed well and incubated for 5 min at room temperature. To stop the reaction 50 ml cold distilled water was added and the cells were immediately pelleted at 4°C, rinsed with 5 ml 1 M sorbitol and frozen at –20°C.

DNA was prepared from the frozen cell pellet by DTAB extraction as previously described (39). Following resuspension of the purified DNA the unmodified DNA samples were subjected to *in vitro* DMS modification as described (40).

For PCR amplification of the DMS-modified genomic DNA, a primer corresponding to the 3′-end of the *URA3* gene in the SCB::*lacZ* plasmid was used: URA3PCR, 5′-ATTTGAGAAG-ATGCGGCCAGC-3′. DNA was first quantitated by measuring A_{260} and ~20 μg/sample were digested with *Apa*I (to facilitate primer annealing). To improve loading differences between samples, DNA digestion and quantitation were checked by agarose gel

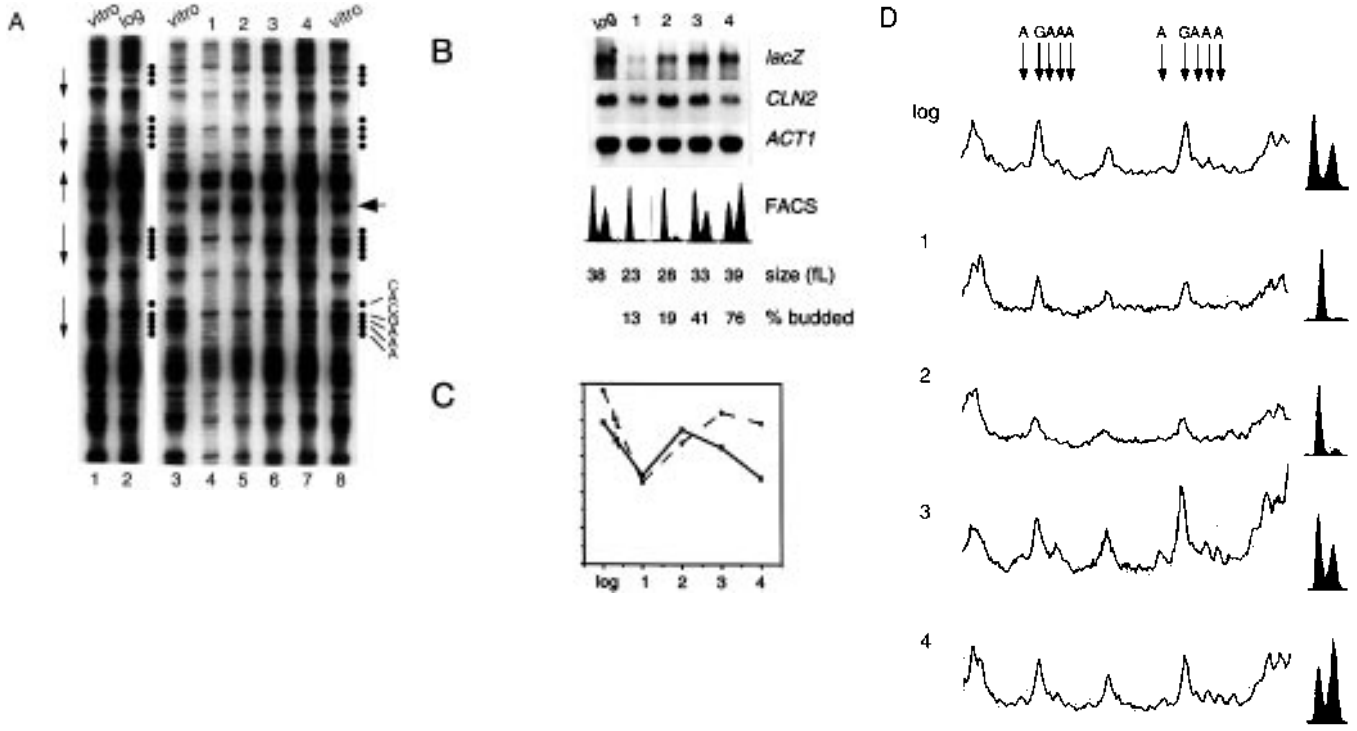

Figure 2. *In vivo* DMS footprinting of SCB sequences in wild-type cells. (**A**) The arrows at left indicate the location and orientation of each SCB sequence and at right is shown the SCB consensus sequence, CACGAAA. The black dots indicate the visible purine residues in the SCB consensus. The large arrow at right indicates the band used to normalize for DNA loading in the phosphorimager plots shown in (D). Lane numbers are indicated at the bottom of the gel. Lanes 1, 3 and 8, *in vitro* DMS-modified DNA from the asynchronous culture (lane 1) and elutriated samples (lanes 3 and 8); lane 2, *in vivo* DMS modification pattern of the asynchronous cell population (log); lanes 4–7, *in vivo* DMS modification pattern of elutriated samples 1–4 as cells progressed from G1 (sample 1) to G2 (sample 4). DMS-modified DNA was PCR amplified as described in Materials and Methods and resolved on an 8% w/v denaturing acrylamide gel. (**B**) Northern analysis of the same samples shown in (A) sequentially probed with *ACT1*, *lacZ* and *CLN2*. Below, the FACS profile, cell size and percent budded cells are shown for each sample (note that percent budded cells was not measured for the 'log' sample). (**C**) Phosphorimager quantitation of the Northern blot shown in (B). The *x*-axis of the graph shows each sample as in (B) and the *y*-axis shows the intensity of each sample in relative phosphorimager units after normalization to *ACT1* mRNA levels. The dashed line represents *lacZ*, the solid line *CLN2*. (**D**) Phosphorimager analysis of the two lower-most SCB sequences as shown in (A). The thin solid line represents the intensity of the bands across the *in vitro* DMS-modified DNA for each sample and the thick solid line the intensity of bands for each *in vivo* DMS-modified sample. In order to normalize lane-to-lane variations in peak intensity the left-most peak in the plot has been set to an arbitrary value of 1000, as described in Materials and Methods. The sequence of the purine residues within each SCB element is shown at the top. FACS profiles are shown at the right of each sample, as in (B). For clarity two of the five SCB sequences are shown, however, the results were the same for the other protected SCB elements (data not shown).

electrophoresis prior to PCR amplification. PCR amplification was carried out under the following conditions: 50 mM KCl, 10 mM Tris–HCl, pH 9.0 (at 25°C), 1% w/v Triton X-100, 0.2 mM each of dATP, TTP, dGTP, dCTP, 0.5 U Taq polymerase (Promega), ~1 pmol ^{32}P-5′-end-labeled primer (37,38). Amplification was carried out for 18 cycles (1 min at 94°C, 2 min at 56°C, 2 min at 76°C per cycle). The products were phenol/chloroform extracted, ethanol precipitated and resolved on an 8% w/v denaturing acrylamide gel. Purified SCB::*lacZ* plasmid was also sequenced using the ^{32}P-end-labeled URA3PCR primer and was run alongside the genomic DNA samples as a marker. The gel was dried and exposed to Kodak XAR-5 film at –70°C or exposed to a Molecular Dynamics PhosphorImager screen.

Phosphorimager analysis

Gels were exposed on a Molecular Dynamics screen and scanned using a Molecular Dynamics PhosphorImager and Imagequant (version 3.1) software. To obtain the graphical representation of the footprints shown in Figures 2, 4, 5 and 6 a line was drawn vertically through the center of the lane and the intensity at each point on the line was integrated by percent area to generate a linear plot of band intensities. To compare the pattern obtained by *in vitro* DMS modification with the pattern obtained by *in vivo* DMS modification samples were normalized for slight differences in DNA quantitation, PCR amplification and gel loading. First, a 'background' line was drawn between the sample lanes (where no DNA was loaded) and the values at each point on this line were subtracted from the values at each equivalent point on the sample line. Second, a band was chosen near the SCB sequences that did not appear to be protected by DMS modification in any experiments and was assigned an arbitrary value of 1000. For example, the raw phosphorimager values for each peak normalized to 1000 in the experiment shown in Figure 2D are as follows (each pair listed as *in vitro* and *in vivo* DMS-modified respectively): log sample, 577.66, 618.74; sample 1, 367.39, 236.98; sample 2, 432.29, 349.95; sample 3, 208.44, 291.14; sample 4, 251.15, 564.88. The phosphorimager plots shown in Figure 6 are taken from the same data as shown in Figures 2, 4 and 5. Only the bottom two SCB sequences are shown for clarity. No consistent protection of 5′ or 3′ flanking sequences was apparent in the phosphorimager plots (data not shown). Several other

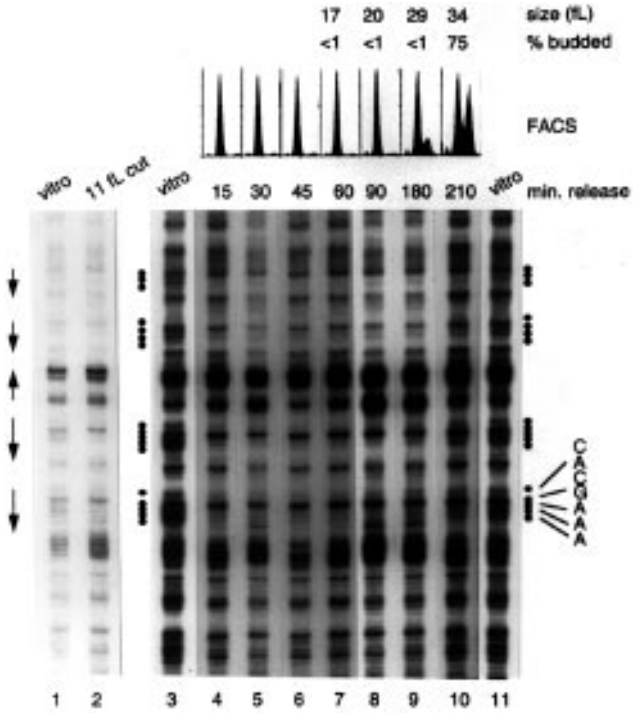

Figure 3. *In vivo* DMS footprinting throughout G1 in a second wild-type strain. The arrows at left indicate the position of the SCB elements and the black dots indicate the resolved purine residues within each SCB. Lane numbers are indicated at the bottom of the gel. Lanes 1 and 2, *in vitro* and *in vivo* DMS modification respectively of the first cut from the elutriation experiment (smallest daughter cells, 11 fl). The pooled G1 cut subsequent to this sample (16 fl) is followed by cell size, percent budded and FACS, as indicated at the top, from 15 to 210 min after release into room temperature media [only the FACS is shown for the 15, 30 and 45 min samples, since cell size (16 fl) and percent budded cells (<1%) remained constant]. Lanes 4–11, *in vivo* DMS modification of cells collected from 15 to 210 min as indicated at top; lanes 3 and 11, *in vitro* DMS modification of two samples from the experiment.

bands, outside the SCB sequences, were also tested as normalization standards and gave similar results (data not shown). The band closest to the SCB sequences was chosen for the final presentation of the data for the following reason. Since Taq polymerase stops at modified purines, there will be a gradient of more intense radioactive bands from the bottom to the top of the gel (the more modified the DNA, the shorter the products). We found that this 'gradient' differed slightly between the *in vitro* and *in vivo* DMS-modified samples (data not shown). Therefore, the farther the normalization band is from the region of interest, the greater the skewing of results toward either the *in vitro* or *in vivo* pattern. This sample-to-sample variation can occur between any modified sample, thus we also chose the SCB-proximal band to compare the *in vivo* DMS patterns shown in Figure 6.

RESULTS

Use of a SCB-dependent *lacZ* reporter plasmid for *in vivo* DMS footprinting

In order to examine binding to SCB sequences *in vivo*, a high copy number plasmid containing five SCB consensus sites inserted upstream of *lacZ* was introduced into yeast cells (Fig. 1). Like chromosomal SBF targets, the tandem SCB elements serve as an orientation-independent enhancer to confer cell cycle regulation of *lacZ* transcription, with maximal expression at Start (9,10). Expression of *lacZ* absolutely depends on the SCB promoter element and is not transcribed in the absence of Swi4 or Swi6 (11,41). Thus high copy expression of the SCB::*lacZ* gene parallels expression of a genomic SCB-dependent promoter, such as *HO*, in both its regulation and transcriptional induction.

Dimethyl sulfate was used for *in vivo* footprinting in order to minimize the perturbation of cells, since treatment times are short (4–5 min) and can be carried out on intact cells at room temperature. Methylated purines were visualized after one-sided PCR amplification using Taq polymerase (37). As a control for the DMS modification pattern in the absence of bound proteins, DNA was isolated from each sample and then subjected to DMS modification *in vitro*, followed by PCR amplification (see Materials and Methods).

Binding of SCB sequences in an asynchronous yeast cell population

A wild-type yeast strain carrying the SCB::*lacZ* plasmid was examined for SCB footprinting during exponential growth. DMS modification of an asynchronous population showed weak protection of the SCB sequences compared with the same DNA sample after deproteinization and *in vitro* DMS modification (Fig. 2A, lanes 1 and 2, and data not shown). In particular, slight protection was observed over the dA residues on the purine-rich strand (5′-CACGAAA-3′) of each SCB sequence (Fig. 2A). There was no significant protection of the pyrimidine-rich strand *in vivo* (5′-GTGCTTT-3′; Fig. 2A, lane 2, and data not shown). The weak protection over the dA residues in the SCB sequences was confirmed by phosphorimager analysis of the *in vivo* DMS-treated sample compared with *in vitro* modified DNA from the same sample (Fig. 2D, 'log').

G1 phase periodicity of SCB protection

Since asynchronous cultures contain cells in both G1 and G2 (by FACS analysis; Fig. 2C), we sought to enrich the SCB footprint by analysis of a homogeneous G1 cell population. G1 daughter cells were obtained by centrifugal elutriation and re-inoculated into conditioned medium. This method minimizes any perturbation of physiological state, since it does not involve temperature shift, media shift or drug addition. Progression of the re-inoculated culture was monitored throughout the cell cycle by cell size, FACS, percentage budded cells and Northern analysis (Fig. 2B and C).

In contrast to the asynchronous population, the homogeneous G1 daughter culture showed significant protection over the SCB sequences in the *lacZ* promoter (Fig. 2A, lanes 4 and 5). Protection of the dA residues within each SCB was more pronounced than in asynchronous cultures (Fig. 2A, compare lanes 2, 4 and 5). In addition, slight protection over the dG residue on the purine-rich strand was also observed (Fig. 2A, lanes 4 and 5). Some residues between the SCB sequences were also slightly protected in G1 cells on the purine-rich strand (Fig. 2A). The dG residues on the pyrimidine-rich strand of the SCB were only weakly footprinted (Fig. 2A, lane 3, and data not shown). As cells progressed into G2 the SCB footprint over these sequences was diminished to a level similar to that observed in the asynchronous population (Fig. 2A, lanes 6 and 7).

Due to technical limitations on the DNA yields of elutriated samples, some of the lanes within one experiment were under-

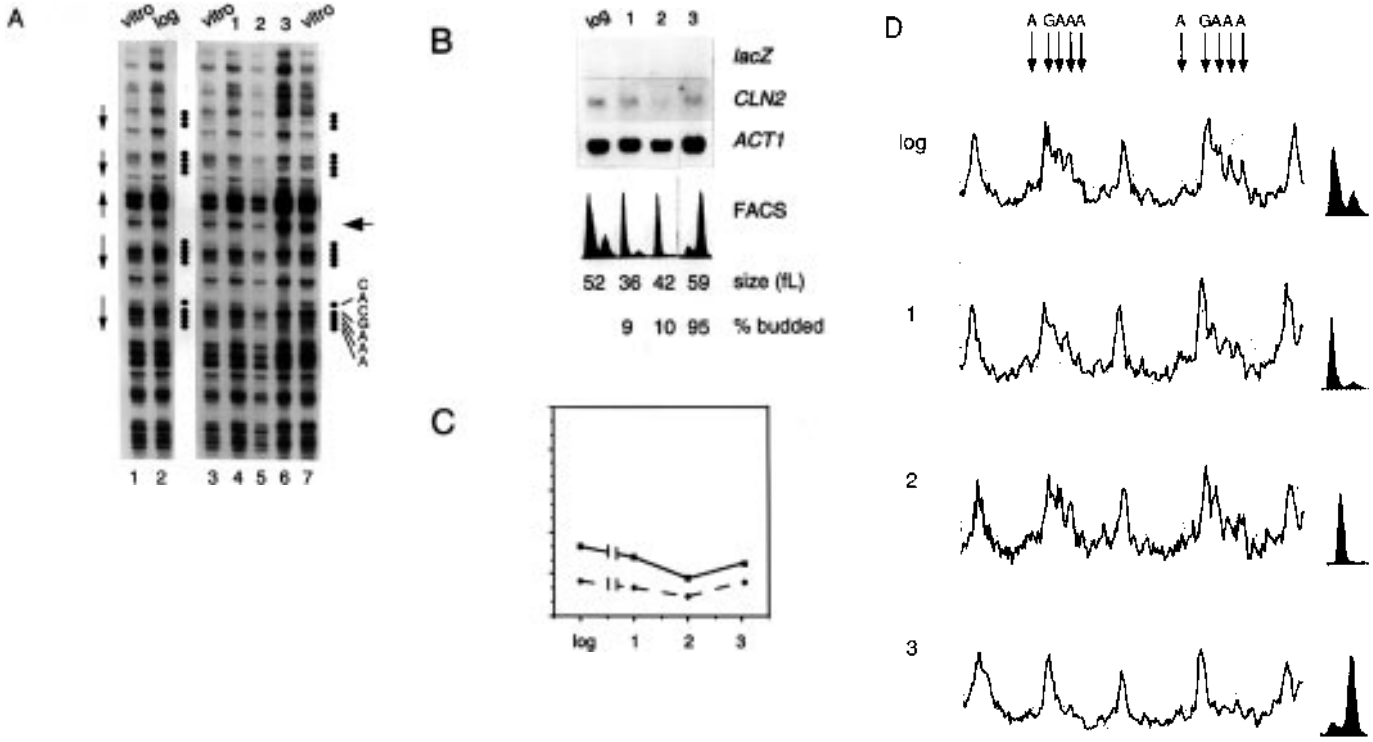

Figure 4. *In vivo* DMS footprinting of SCB sequences in a *swi4* deletion strain. This strain is isogenic to the wild-type strain shown in Figure 3. The arrows at left indicate the position of the SCB elements and the black dots indicate the resolved purine residues within each SCB. Lane numbers are indicated at bottom. (**A**) Lanes 1, 3 and 7, *in vitro* DMS-modified DNA from log phase (lane 1) and elutriated samples (lanes 3 and 7); lane 2, *in vivo* DMS modification pattern of an exponentially growing cell population (log); lanes 4–6, *in vivo* DMS modification pattern of samples 1–3 as cells progressed from G1 (sample 1) to G2 (sample 3). (**B**) Northern analysis of the same samples shown in (A) sequentially probed with *ACT1*, *lacZ* and *CLN2*. Below, the FACS profile, cell size and percent budded cells are shown for each sample (percent budded was not determined for the 'log' sample). (**C**) Phosphorimager quantitation of the Northern blot shown in (B). The graph is in arbitrary phosphorimager units on the same scale as in Figure 2C. The dashed line represents *lacZ* and the solid line *CLN2* after normalization to *ACT1* mRNA levels. (**D**) Phosphorimager analysis of the two lower-most SCB sequences as shown in (A). The thin solid line represents the intensity of the bands across the *in vitro* DMS-modified DNA for each sample and the thick solid line the intensity of bands for each *in vivo* DMS-modified sample. For clarity two of the five SCB sequences are shown, however, the results were the same for the other protected SCB elements (data not shown).

loaded relative to others (Fig. 2A, compare lanes 2 and 4). For this reason, DMS modification was also carried out on deproteinized DNA for each sample and normalized to the *in vivo* DMS modification pattern using a phosphorimager (see Materials and Methods). For example, phosphorimager analysis of the weak protection apparent in the residues below the SCB sequences (close to *URA3*; Fig. 2A, lanes 4 and 5) showed that this protection was not cell cycle specific (Materials and Methods and data not shown). However, the phosphorimager plots did confirm the weak protection over the dA residues in the SCB for the asynchronous cell population (Fig. 2D, 'log'). In the G1 samples, strong protection over dA and dG residues of the SCB was also observed after phosphorimager normalization, including weak protection over two adjacent purine residues between the SCBs (Fig. 2D, panels 1 and 2). As cells progressed into G2 this protection declined significantly (Fig. 2D, panel 4).

Northern analysis showed that the peak of *lacZ* transcription in G1 coincided with or followed closely after footprinting over the SCB region (Fig. 2B and C). The induction of *lacZ* transcription showed parallel kinetics to another SCB-dependent gene, *CLN2* (Fig. 2C). The *lacZ* transcript peaked slightly later than *CLN2* and its level persisted compared with *CLN2* mRNA (Fig. 2C), possibly due to differences in mRNA half-life. The large samples required within each experiment did not allow us to follow the transcripts further into the cell cycle. However, similar kinetics of *lacZ* and *CLN2* induction were also observed in another elutriation (data not shown).

A similar pattern of DMS protection was observed in all G1 cell populations, whether in early or late G1 (Fig. 3). For example, the footprinting pattern in small daughter cells (11 fl), although of weak intensity due to the small sample size, did not significantly differ from the pattern in larger G1 cells (Fig. 3, lanes 2 and 4–7). One minor difference observed was that protection of the dG residue of the SCB was more pronounced in cells in mid-G1 compared with early G1 or asynchronous cultures (Fig. 3). As cells entered G2, protection over the SCB sequences was diminished (Fig. 3, lanes 9 and 10). For example, cells that were 75% budded showed almost no footprint as compared with an *in vitro* DMS-modified sample (Fig. 3, lanes 10 and 11).

Requirement of both *SWI4* and *SWI6* for SCB binding *in vivo*

To determine whether the *in vivo* SCB footprint was due to SBF or some other DNA binding factor we examined protection of SCB sequences throughout the cell cycle in strains that were deleted of *SWI4* or *SWI6*. *SWI4* and *SWI6* disruption strains were each elutriated and examined for DMS footprinting *in vivo*. In

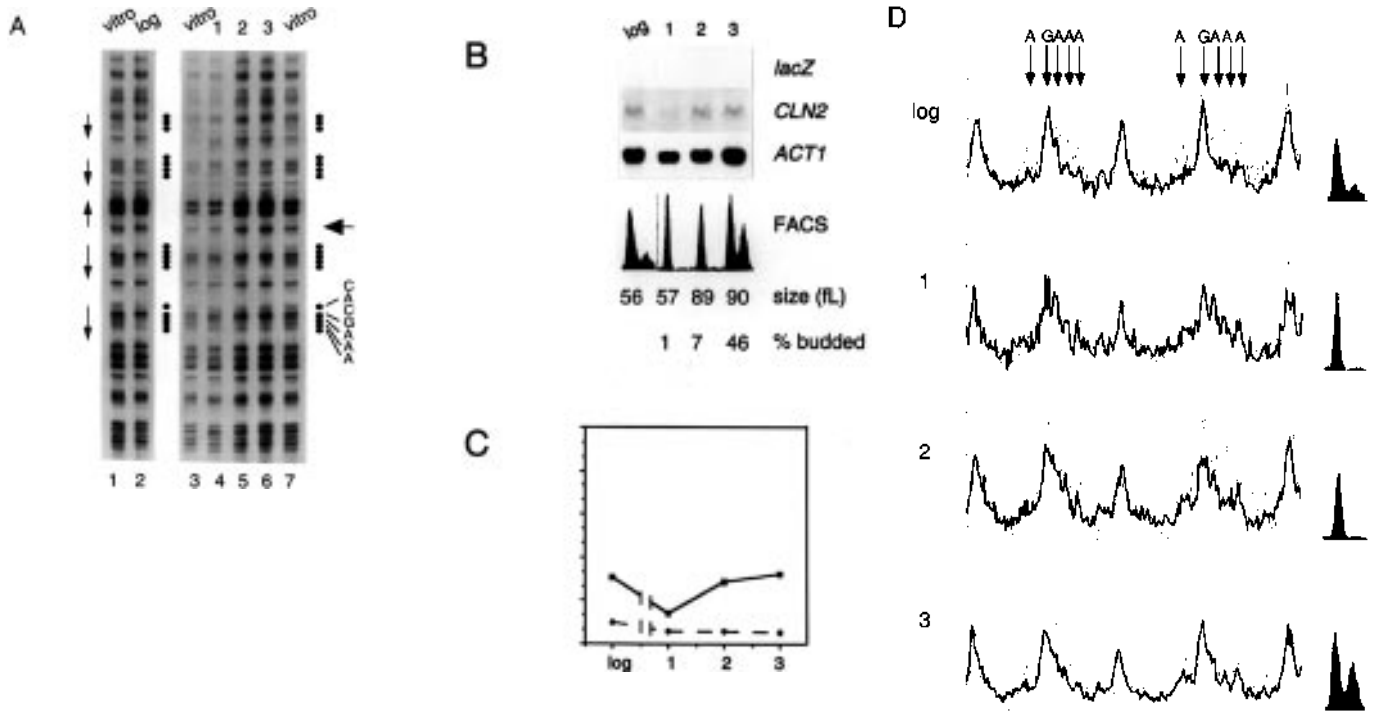

Figure 5. *In vivo* DMS footprinting of SCB sequences in a *swi6* deletion strain. This strain is isogenic to the wild-type strain shown in Figure 3. The arrows at left indicate the position of the SCB elements and the black dots indicate the resolved purine residues within each SCB. Lane numbers are indicated at bottom. (**A**) Lanes 1, 3 and 7, *in vitro* DMS-modified DNA from log phase (lane 1) and elutriated samples (lanes 3 and 7); lane 2, *in vivo* DMS modification pattern of an exponentially growing cell population (log); lanes 4–6, *in vivo* DMS modification pattern of samples 1–3 as cells progressed from G1 (sample 1) to G2 (sample 3). (**B**) Northern analysis of the same samples shown in (A) sequentially probed with *ACT1*, *lacZ* and *CLN2*. Below, the FACS profile, cell size and percent budded cells are shown for each sample (percent budded was not determined for the 'log' sample). (**C**) Phosphorimager quantitation of the Northern blot shown in (B). The graph is in arbitrary phosphorimager units and on the same scale as in Figure 2C. The dashed line represents *lacZ* and the solid line *CLN2* after normalization to *ACT1* mRNA levels. (**D**) Phosphorimager analysis of the two lower-most SCB sequences as shown in (A). The thin solid line represents the intensity of the bands across the *in vitro* DMS-modified DNA for each sample and the thick solid line the intensity of bands for each *in vivo* DMS-modified sample. For clarity two of the five SCB sequences are shown, however, the results were the same for the other protected SCB elements (data not shown).

contrast to wild-type cells, no significant footprint over the SCB sequences was observed in either deletion strain at any stage in the cell cycle (Figs 4A and 5A). Northern analysis of elutriated cells from both *SWI4* and *SWI6* deletion strains showed that *lacZ* was not transcribed at any stage of the cell cycle (Figs 4B and C and 5B and C). However, as has been seen previously, low levels of *CLN2* were still expressed in the absence of *SWI4* or *SWI6* (Figs 4B and C and 5B and C; 21,22).

Phosphorimager analysis was performed on the *in vivo* footprinting patterns for both the *swi4*Δ and *swi6*Δ elutriation experiments (Figs 4D and 5D). In *swi4*Δ cells no detectable footprint was observed in either the asynchronous population, G1 or G2 cells (Fig. 4D). In *swi6*Δ cells no detectable footprint was seen in any elutriated sample (Fig. 5D). The very weak footprint observed over the dA residues in the *swi6*Δ asynchronous cell population (Fig. 2D, panel 1) was not observed in other experiments or in the purified G1 or G2 samples from this experiment (Fig. 5D, panels 2–4, and data not shown).

We also directly compared the *in vivo* DMS modification patterns for wild-type, *swi4*Δ and *swi6*Δ cells between G1 cells and cells that had entered G2 (Fig. 6). In wild-type cells there was a clear protection of SCB sequences in the G1 cells compared with cells that had progressed through Start, both visually and by phosphorimager analysis (Fig. 6A). In *swi4* or *swi6* deletion strains, however, there was no detectable difference between the *in vivo* DMS modification patterns in G1 cells compared with cells later in the cell cycle (Fig. 6B and C).

DISCUSSION

Binding to tandem SCB sequences and cell cycle regulation

We chose centrifugal elutriation and DMS footprinting to analyze the cell cycle regulation of SCB binding *in vivo*. We found that footprinting over SCB sequences was specifically detected in G1 daughter cells purified by centrifugal elutriation and was not detected in cells that had progressed into G2. Although the least physiologically perturbing, cell sampling by elutriation usually precludes analysis beyond one cell cycle. In contrast, other methods involving cell cycle arrest and release can typically retain synchrony for two cell cycles. However, we found only a weak footprint at SCB sequences in wild-type cells using several methods of cell cycle arrest, including α-factor, nocodazole and temperature-sensitive *cdc28* alleles (data not shown).

The technical difficulty of obtaining enough DNA from each cell cycle sample for DMS footprinting also necessitated the use of a high copy number plasmid. For example, in these experiments

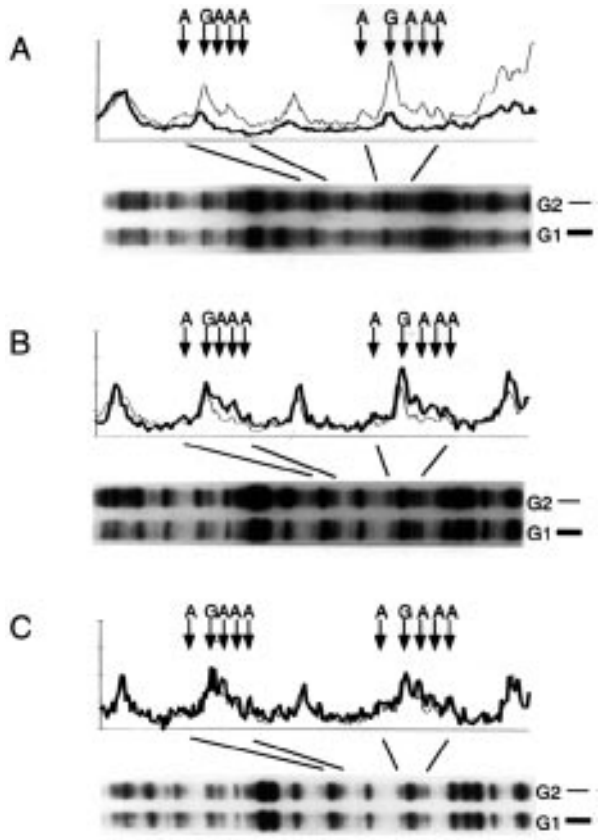

Figure 6. Phosphorimager analysis of *in vivo* DMS footprinting from G1 and G2 cell populations in wild-type, *swi4*Δ and *swi6*Δ cells. The purines in each SCB repeat are indicated at the top. (**A**) *In vivo* DMS modification patterns between samples 2 and 3 from Figure 2A were directly compared. The plots are normalized to the same SCB-proximal band as shown in Figure 2A. The thick line represents the scan of the G1 cells (see Fig. 2A, lane 5), the thin line that of cells entering G2 (Fig. 2A, lane 6). (**B**) *In vivo* DMS modification patterns were compared for *swi4*Δ cells in G1 (thick line; see Fig. 4A, lane 4) and G2 (thin line; see Fig. 4A, lane 6). (**C**) *In vivo* DMS modification patterns for *swi6*Δ cells in G1 (thick line; see Fig. 5A, lane 5) and as cells entered G2 (thin line; see Fig. 5A, lane 6).

single copy genomic footprinting would require ~1 l of purified, elutriated cells for each cell cycle time point. While ligation-mediated PCR (LM-PCR) analysis has been successfully used in yeast for *in vivo* footprinting of single copy genomic sequences (40), we were unable to detect an SCB footprint with LM-PCR (data not shown). It is possible that the number of protected sequences was too low to be detected after ligation and PCR amplification. High copy number plasmids were also used in initial studies of cell cycle-regulated binding of the origin recognition complex, ORC, at ARS1 (42,43).

The specificity of SBF binding *in vivo*

Using *in vivo* DMS modification we observed protection of several purines in the SCB promoter during G1. Most pronounced was protection of the dA residues of the SCB, CACGAAA, whereas the only remaining purine, dG, was weakly protected in G1. *In vitro* the carboxymethylation interference pattern of the N-terminus of Swi4 bound to the *CLN2* SCB shows a very similar footprinting pattern (15). Four of the five SCB sequences on one strand were all protected in G1, including two purine residues between the SCB sequences. Previous studies have suggested that SBF can bind cooperatively to tandem SCB sequences (11), however, since the DMS footprinting pattern represents a population of DNA molecules, we cannot determine SBF occupancy on any particular SCB element.

The absence of SCB binding in a *swi4* deletion strain supports the hypothesis that it is SBF that is bound to the promoter and not some other DNA binding factor, such as MBF. MBF complexes contain Swi6 and the Swi4 homolog Mbp1 (reviewed in 8). *In vitro* Mbp1 and Swi4 can bind to the same sequences and binding of SBF to the SCB can be specifically competed by MCB sequences (24,25). Since Mbp1 is still present in the *SWI4* deletion strain, we presume that the specificity of binding of MBF and SBF is more tightly regulated *in vivo* and that MBF cannot substitute for binding to the SCB sequences in the absence of Swi4. A recently identified factor, SCELA (*S.cerevisiae* E2F-like activity), can efficiently bind SCB sites *in vitro* (44). Our results suggest that SCELA does not detectably bind SCB sequences *in vivo*.

We have found that Swi4 protein alone cannot bind SCB sequences *in vivo*. *In vitro* the N-terminal DNA binding domain of Swi4 is sufficient to footprint an SCB consensus sequence in the *CLN2* promoter (15). However, in our experiments protection of SCB sequences was not detected in *swi6*Δ cells. A regulatory mechanism may prevent binding of Swi4 alone to the SCB sequences in G1. Since Swi6 protein is found predominantly in the nucleus only in G1, it is possible that Swi6 nuclear localization is important for SBF complex formation (13,48).

SCB binding *in vivo* may not be sufficient for G1 transcription

Although the SCB sequences upstream of the G1 cyclins *CLN1* and *CLN2* are required for their maximum expression at Start, recent studies have indicated that cell cycle regulation of these genes is not strictly dependent on upstream SCB sites (21,22). In particular, deletion of the SCB and MCB elements upstream of *CLN2* does not completely abolish its periodic expression (21,22). Similarly, deletion of three upstream MCB elements does not abolish the G1 periodicity of *SWI4* mRNA (26). Thus SBF and MBF may be only partially responsible for the amplification of G1 cyclin levels at Start. We have shown a correlation between the timing of SCB binding *in vivo* and transcriptional activation of a reporter gene that is completely SBF dependent. Whether the role of SBF is to help initiate transcription or amplify it, binding of SCB sequences at the time of *CLN* transcriptional induction is consistent with a role for SBF binding in the initial induction of SCB target genes in early G1. However, since SCB sequences were also occupied in early G1, prior to the peak in SCB-driven transcription, it is possible that a second event after SCB binding may be required for transcriptional induction.

The regulation of SCB binding *in vivo*

The fact that SCB binding is G1 specific raises the interesting question as to what activates the binding of SBF in early G1 and what events must occur, if any, after SBF binding to activate transcription. Several studies have shown that transcriptional activation of the G1 cyclins and *HO* are dependent on active Cdc28 kinase (reviewed in 8). In particular, recent experiments show that SBF- and MBF-driven transcription of the G1 cyclins is activated by the Cln3–Cdc28 kinase (45,46). Our finding that

SCB binding occurs specifically in G1 suggests that the DNA binding activity of SBF may be a direct target for such regulation. Other studies have suggested an additional role for Cdc28 in regulating SBF activity. In particular, it has previously been shown that Clb2–Cdc28 kinase is required for repression of cyclin expression in G2 and that Clb2 can bind Swi4 (47). These results suggest that Clb2–Cdc28 may negatively regulate G1 cyclin expression by direct interaction with Swi4. Our finding that SCB sites are not significantly occupied in G2 is consistent with the possibility that Swi4 regulation by Clb2–Cdc28 kinase may occur at the level of SCB binding *in vivo*.

Note added in proof

A second study has revealed cell cycle-regulated binding to SCB sequences *in vivo*. Koch *et al*. find G1-specific binding of SCB sequences within the *CLN2* promoter *in vivo* [Koch,C., Schleiffer,A., Ammerer,G. and Nasmyth,K. (1995) *Genes Dev.* in press].

ACKNOWLEDGEMENTS

We are indebted to M. Tyers for suggestions and help with initial elutriations. We are grateful to C. Koch and K. Nasmyth for helpful discussions and for communicating results prior to publication. For critical comments we thank C. Greider, A. Spence, P. Sadowski, M. Tyers and members of the laboratory. We thank C. Smith for assistance with FACS analysis, R. Collins and T. Beattie for advice regarding phosphorimager quantitation, J. Wei for computer assistance and B. Bolychuk and P. Schwartz for photography. LH was a post-doctoral fellow of the National Cancer Institute of Canada. This work was supported by a grant from the Medical Research Council of Canada to BJA. BJA is a Medical Research Council of Canada Scholar.

REFERENCES

1 Nasmyth,K. (1993) *Curr. Opin. Cell Biol.*, **5**, 166–179.
2 Tyers,M., Tokiwa,G. and Futcher,B. (1993) *EMBO J.*, **12**, 1955–1968.
3 Wittenberg,C., Sugimoto,K. and Reed,S. (1990) *Cell*, **62**, 225–237.
4 Ogas,J., Andrews,B.J. and Herskowitz,I. (1991) *Cell*, **66**, 1015–1026.
5 Fernandez,S.M.J., Sutton,A., Zhong,T. and Arndt,K.T. (1992) *Genes Dev*, **6**, 2417–2428.
6 Measday,V., Moore,L., Ogas,J., Tyers,M. and Andrews,B. (1994) *Science*, **266**, 1391–1395.
7 Espinoza,H., Ogas,J., Herskowitz,I. and Morgan,D. (1994) *Science*, **266**, 1388–1391.
8 Koch,C. and Nasmyth,K. (1994) *Curr. Opin. Cell Biol.*, **6**, 451–459.
9 Breeden,L. and Nasmyth,K. (1985) *Cold Spring Harbor Symp. Quant. Biol.*, **50**, 643–650.
10 Breeden,L. and Nasmyth,K. (1987) *Cell*, **48**, 389–397.
11 Andrews,B.J. and Herskowitz,I. (1989) *Cell*, **57**, 21–29.
12 Andrews,B.J. and Herskowitz,I. (1989) *Nature*, **342**, 830–833.
13 Taba,M.R.M., Muroff,I., Lydall,D., Tabb,G. and Nasmyth,K. (1991) *Genes Dev.*, **5**, 2000–2013.
14 Andrews,B.J. and Moore,L.A. (1992) *Proc. Natl. Acad. Sci. USA*, **89**, 11852–11856.
15 Primig,M., Sockanathan,S., Auer,H. and Nasmyth,K. (1992) *Nature*, **358**, 593–597.
16 Sidorova,J. and Breeden,L. (1993) *Mol. Cell. Biol.*, **13**, 1069–1077.
17 Breeden,L. and Mikesell,G.E. (1991) *Genes Dev.*, **5**, 1183–1190.
18 Nasmyth,K. (1985) *Cell*, **42**, 225–235.
19 Dirick,L. and Nasmyth,K. (1991) *Nature*, **351**, 754–757.
20 Lowndes,N.F., Johnson,A.L., Breeden,L. and Johnston,L.H. (1992) *Nature*, **357**, 505–508.
21 Cross,F.R., Hoek,M., McKinney,J.D. and Tinkelenberg,A.H. (1994) *Mol. Cell. Biol.*, **14**, 4779–4787.
22 Stuart,D. and Wittenberg,C. (1994) *Mol. Cell. Biol.*, **14**, 4788–4801.
23 Koch,C., Moll,T., Neuberg,M., Ahorn,H. and Nasmyth,K. (1993) *Science*, **261**, 1551–1557.
24 Dirick,L., Moll,T., Auer,H. and Nasmyth,K. (1992) *Nature*, **357**, 508–513.
25 Lowndes,N.F., Johnson,A.L. and Johnston,L.H. (1991) *Nature*, **350**, 247–250.
26 Foster,R., Mikesell,G.E. and Breeden,L. (1993) *Mol. Cell. Biol.*, **13**, 3792–3801.
27 Schwob,E. and Nasmyth,K. (1993) *Genes Dev.*, **7**, 1160–1175.
28 Verma,R., Smiley,J., Andrews,B. and Campbell,J.L. (1992) *Proc. Natl. Acad. Sci. USA*, **89**, 9479–9483.
29 Lowndes,N.F., McInerny,C.J., Johnson,A.L., Fantes,P.A. and Johnston,L.H. (1992) *Nature*, **355**, 449–53.
30 Reymond,A., Marks,J. and Simanis,V. (1993) *EMBO J.*, **12**, 4325–4334.
31 Andrews,B.J. and Mason,S.W. (1993) *Science*, **261**, 1543–1544.
32 Lowndes,N.F. and Johnston,L.H. (1992) *Trends Genet.*, **8**, 79–81.
33 Gietz,D., Jean,A.S., Woods,R.A. and Schiestl,R.H. (1992) *Nucleic Acids Res.*, **20**, 1425.
34 Guthrie,C. and Fink,G. (1991) *Guide to Yeast Genetic and Molecular Biology.* Academic Press, New York, NY.
35 Tyers,M., Tokiwa,G., Nash,R. and Futcher,B. (1992) *EMBO J.*, **11**, 1773–1784.
36 Hadwiger,J.A., Wittenberg,C., Richardson,H.E., Lopes,M.d.B. and Reed,S.I. (1989) *Proc. Natl. Acad. Sci. USA*, **86**, 6255–6259.
37 Axelrod,J.D. and Majors,J. (1989) *Nucleic Acids Res.*, **17**, 171–183.
38 Keleher,C.A., Redd,M.J., Schultz,J., Carlson,M. and Johnson,A.D. (1992) *Cell*, **68**, 709–719.
39 Burns,N., Grimwade,B., Ross-Macdonald,P.B., Choi,E.-Y., Finberg,K., Roeder,G.S. and Snyder,M. (1994) *Genes Dev.*, **8**, 1087–1105.
40 Ganter,B., Tan,S. and Richmond,T.J. (1993) *J. Mol. Biol.*, **234**, 975–987.
41 Andrews,B.J. and Moore,L. (1992) *Biochem. Cell Biol.*, **70**, 1073–1080.
42 Diffley,J.F., Cocker,J.H., Dowell,S.J. and Rowley,A. (1994) *Cell*, **78**, 303–316.
43 Rowley,A., Cocker,J.H., Harwood,J. and Diffley,J.F.X. (1995) *EMBO J.*, **14**, 2631–2641.
44 Vemu,S. and Reichel,R. (1995) *J. Biol. Chem.*, **270**, 20724–20729.
45 Dirick,L., Bohm,T. and Nasmyth,K. (1995) *EMBO J.*, **14**, 4803–4813.
46 Stuart,D. and Wittenberg,C. (1995) *Genes Dev.*, **9**, 2780–2794.
47 Amon,A., Tyers,M., Futcher,B. and Nasmyth,K. (1993) *Cell*, **74**, 993–1007.
48 Sidorova,J., Mikesell,G. and Breeden,L. (1995) *Mol. Biol. Cell*, **6**, 1641–1658.